

Atmospheric Full Scale Testing of a Morphing Trailing Edge Flap System for Wind Turbine Blades

Thanasis K. Barlas, Helge A. Madsen

Abstract—A novel Active Flap System (AFS) has been developed at DTU Wind Energy, as a result of a 3-year R&D project following almost 10 years of innovative research in this field. The full scale AFS comprises an active deformable trailing edge has been tested at the unique rotating test facility at the Risø Campus of DTU Wind Energy in Denmark. The design and instrumentation of the wing section and the AFS are described. The general description and objectives of the rotating test rig at the Risø campus of DTU are presented, along with an overview of sensors on the setup and the test cases. The post-processing of data is discussed and results of steady, flap step and azimuth control flap cases are presented.

Keywords—morphing, adaptive, flap, smart blade, wind turbine.

I. INTRODUCTION

THE size of wind turbines has been increasing rapidly over the past years. Rotors of more than 160m in diameter are already commercially available. Focusing on lowering the cost per kWh, new trends and technological improvements have been primary targets of research and development. One main focus is on developing new technologies, which are, amongst other, capable of considerably reducing fatigue loads on wind turbines. New concepts for dynamic load reduction are focusing on a much faster and detailed load control, compared to existing individual blade pitch control, by utilizing active aerodynamic control devices distributed along the blade span. The concepts so far have focused on the combination of actuators, aerodynamic surfaces such as flaps, sensors and controllers, which can provide dynamic load control. Such concepts are generally referred to as smart rotor control, a term used in rotorcraft research, and investigated for wind turbine applications over the past years in terms of conceptual and aeroelastic analysis and small scale wind tunnel experiments and recently field testing [5]. For a review of the state-of-the-art in the topic, the reader is referred to [2]. So far, results from numerical and experimental analysis mostly focusing on trailing edge flaps, have shown a considerable potential in fatigue load reduction. Although, small scale blade and rotor experiments have utilized piezoelectric bender actuator concepts to provide deformable trailing edge activation, such concepts are considered not directly up-scalable for modern large scale wind turbine blades, without any additional mechanical amplification parts. The lack of technology solutions for flap control for wind turbines initiated a development work at Risø Campus of DTU Wind Energy in 2006 with the main

Thanasis K. Barlas and Helge A. Madsen are with the Aeroelastic Design section, Department of Wind Energy, Technical University of Denmark (DTU), Roskilde, 4000, Denmark e-mail: tkba@dtu.dk and hama@dtu.dk.



Fig. 1. The rotating rig test stand

objective to develop a robust and efficient flap system for implementation on MW scale turbines. This led to the design of the Controllable Rubber Trailing Edge Flap (CRTEF). The initial design studies led to the basic concept of a trailing edge flap manufactured in an elastic material such as e.g. rubber or plastic and with suitable reinforced voids that can be pressurized with a medium such as air or a liquid and in this way give the desired deflection of the flap. In the INDUFLAP project (Industrial adaptation of a prototype flap system for wind turbines) the Active Flap System (AFS) has been further developed towards industrial application, also focusing of full scale prototype testing ([1], [3], [4]).

The focus of this article is to present the results of the AFS testing in the rotating rig facility at DTU. Testing the performance and robustness of the smart blade technology is an important part of the INDUFLAP project. Wind tunnel testing of an earlier prototype flap system was performed in 2009 and proved that the actuation concept works in a wind tunnel [1]. However, there is big step from wind tunnel testing on a stationary blade section to full scale turbine application and therefore a so-called rotating test rig has been developed in the INDUFLAP project (Fig. 1).

The idea behind the test rig is that the testing should be as

close as possible to the rotating test environment on the real turbine and have the same unsteady inflow conditions and a size of the flap close to a full scale application. This has been obtained by manufacturing a blade section with a 1m chord and 2.2m span and mounting it on a 10m long boom on the rotating rig. The basic platform for the rotating test rig is the 100kW Tellus turbine positioned at the old turbine test site at DTU, Campus Risø. The original three bladed rotor has been taken down and a new full variable speed drive has been installed so the rotational speed with the boom mounted is controllable between 0 and 60 rpm (Fig. 1). A comprehensive instrumentation of the test rig has been carried out and includes sensors for the blade surface pressure distribution on the mid span position, which enable a continuous monitoring of the instantaneous sectional aerodynamic loading on blade, and thus also allow measuring the exact response of flap actuation. Another part of the instrumentation comprises two five-hole pitot tubes of the leading edge of the blade section for measuring the inflow to the blade. Finally, metrological data such as wind speed and wind direction is measured in three heights in a nearby met mast.

Main characteristics of the flap tests:

- Proof of concept of the flap system in atmospheric conditions
- Measurement of aerodynamic characteristics in free wind as an important supplement to wind tunnel measurements on aerofoil sections
- Scale of flap system and blade section close to real scale
- Potential of load reduction with flap actuation in a realistic scale

II. WING SECTION AND FLAP SYSTEM DESIGN

The wing section based on the shape of a NACA0015 aerofoil has been manufactured in-house with a constant chord length of 1m. The overall concept consists of a spanwise 2.2 meter long wing section covered with side pods in each end giving a total length of 3.4 meter. The section is based on an inner aluminum structure covered with two shells of glass-epoxy composite material. The aluminum structure consists of an 110mm hollow tube, two spante structures and a U-profile web. The aluminum parts were welded together. The tube makes it possible to mount and dismount the wing section on a boom and the U-profile web at the trailing edge is for fixation of different morphing rubber flaps. The section is equipped with three pressure tanks, valves, control units, data acquisition equipment, and 200 pressure holes connected with individual rubber tubes for pressure measurement on strategic places on the aerofoil. Two 5-hole Pitot tubes are also mounted for inflow measurements.

The basic design of the flap is made of a flexible polymer material with suitable reinforced voids that can be pressurized with a medium such as air or a liquid and in this way give the desired deflection of the flap [4]. The design space has been explored utilizing Finite Element (FE) modeling of cavity configurations, exploring various void arrangements,



Fig. 2. The wing section with the flap mounted on the rotating rig test stand



Fig. 3. View of the wing-flap section

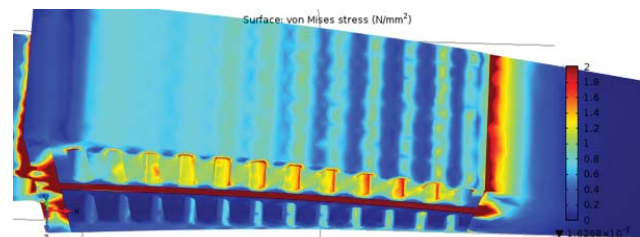


Fig. 4. Design of AFS based on F.E. model [4]

and internal reinforcement structure concepts. The final design achieved the targets for the flap cavity designs regarding:

- stress level within material tolerance
- maximum flap tip deflection
- cavity wall tolerances vs. production cost

The flap powering system, which is developed and implemented by Hydratech Industries, comprises a pneumatic system providing pressurized air into the voids of the flexible part of the flaps. A compressor supplies pressurized air into 3 accumulators, where the pressure is regulated through regulator valves into low, medium, and high pressure. A series of 3 switches per flap side ('positive'-upper, 'negative'-lower) control which of the three pressure levels is connected to the flap voids (on-off). A fourth switch per flap side controls the release of pressure. Controlling the switch valves allows for dynamic control of the pressure in the voids and therefore the flap deflection. The pressure at the flap inlets, the switches, the accumulators and the compressor are measured using

TABLE I
MEASUREMENT SENSORS.

sensor	units
Pitch angle	deg
Positive flap angle	bar
Negative flap angle	bar
Inflow angle pressure difference Pitot tube (P45)	psi
Dynamic pressure Pitot tube (P16)	psi
Root flapwise strain	mV/V
Root edgewise strain	mV/V
Blade section flapwise strain	mV/V
Blade section edgewise strain	mV/V
Pressure from chordwise taps	psi
Rotor speed	rpm
Rotor azimuth	deg
Yaw position	deg
Wind speed from met mast at 29m	m/s
Wind direction from met mast at 29m	m/s

pressure transducers.

In this measurement campaign, signals from various sensors on the rotating rig and the met mast are recorded.

Data channels involve sensor signals related to

- operation of rotating rig
- inflow
- flap operation
- blade section aerodynamics
- boom and blade section structural response

In total, 196 data channels are recorded. The sensor signals in use have been converted from a raw signal (usually [V]) into a physical quantity already within the acquisition software processing. In some of the sensors further calibration /post processing is used in order to derive physical quantities of interest (e.g. flap deflection angle from flap pressure).

III. TEST CASES

The first cases comprise 10min time series with steady pitch (0-20 degrees) and flap settings (zero, min, max angle). The next cases include a slow square signal activation of the flap at 0.05Hz towards its maximum/minimum deflection range. The last cases concern prescribed harmonic flap control based at 0.33Hz on the azimuth angle. Due to the fact that the implemented pitch system could only reach a range of 1-25 degrees towards stall in an upwind orientation, all tests were performed in a downwind orientation, in order to operate within an inflow angle range of interest. All cases are performed with a constant rotor speed of 20 rpm.

The integrated aerodynamic forces at the wing section are calculated from the pressure hole measurements on the aerofoil, also utilizing the Pitot tube pressure measurements. In one part of the post-processing the local flow angle and dynamic pressure (and local flow velocity) are derived from the Pitot tube pressure differences. In the other part of the post-processing, the chordwise pressure tap data is utilized and corrected in order to derive the integrated aerodynamic forces (and further coefficients).

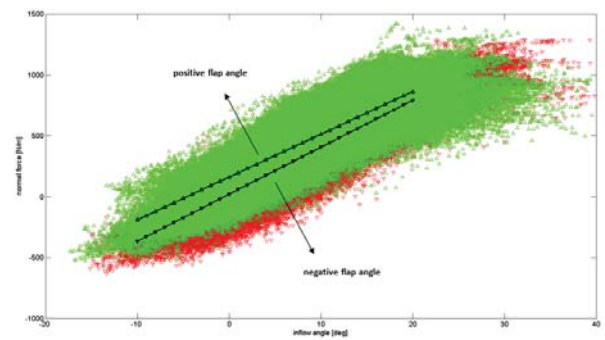


Fig. 5. Normal force for every sample plotted with corresponding calculated inflow angle (green triangles: positive max flap, red triangles: negative flap max, black triangles with solid green triangles: linear fit for positive max flap, black triangles with solid red triangles: linear fit for negative max flap).

IV. RESULTS

The pressure post-processing is implemented and derived variables for every time step are statistically analyzed. The inflow angle and normal force are calculated using the pressure data and the results for every sample are processed. In the linear region both the scatter data and the linear fit data show the expected tendency of positive flap angles resulting in larger normal force and negative flap angles resulting in smaller normal force. The scatter of data due to changing operating conditions, though results in some uncertainty. Using the flap calibration and the calculated values, an estimation of the average flap performance compared to the pitch performance can be performed:

$$\partial F_N / \partial \delta = 0.32 \partial F_N / \partial \alpha$$

where F_N the integral normal force on the section, δ the flap angle and α the inflow angle

The average change in normal force due to a degree change in flap angle then results in 32% of the average change in normal force due to a degree change in inflow angle. This compares well with the performance of the earlier flap prototypes tested in a wind tunnel [1]. The results of the steady cases are shown in Fig. 5.

For the case of square flap input signals, the derived aerodynamic data is averaged over smaller periods during the flap activation cycle. In all cases a square input of 0.05 Hz is used, so the flap activation cycle is divided into 4 sections of 5s each. The positive flap region is defined as the 2nd section and the negative flap region is defined as the 4th section. This is shown with a green line (positive flap) and a red line (negative flap) in Fig. 6. It is seen that the pressure on the flap shows a reasonable rise time, but the settling time to the steady state extreme values is long, due to the limitations of the pneumatic system (size of accumulators

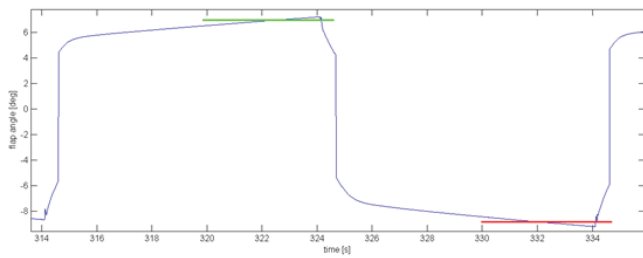


Fig. 6. Flap square signal activation cycle showing defined positive/negative regions.

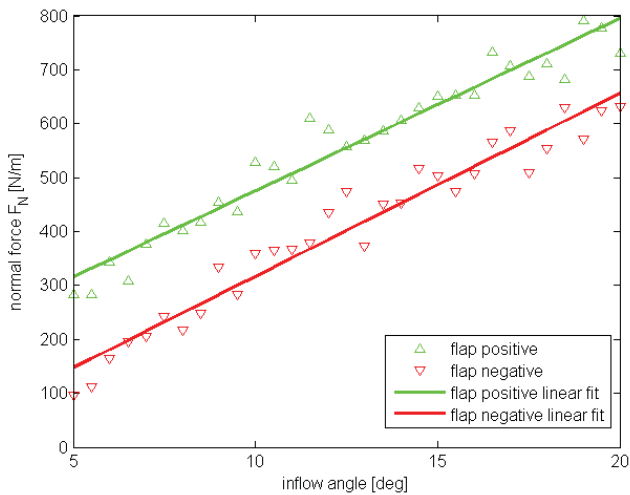


Fig. 7. Normal force data for extreme flap positions plotted against inflow angle. Data averaged every 0.5deg inflow angle.

and use of compressor. Every case is first processed and derived aerodynamic variables are analyzed without time averaging in a 10-min time series. For the case of square flap input signals, the derived aerodynamic data is averaged over the defined flap regions in each flap cycle. For each of these 5s samples the pressure distribution and the Pitot tube pressure signals are averaged and aerodynamic variables are calculated. Firstly, the normal force values for the extreme flap positions are binned based on the pitch setpoint. As expected, increasing the pitch angle (pitching to feather in the downwind configuration) results in reduced normal force. Moreover, for every pitch setpoint a consistent average change in normal force is shown for the flap extremes, despite the scatter of data due to changing inflow. In Fig. 7 the data at each of the two flap extremes is averaged for every inflow angle and a linear curve is fitted. The average change in normal force due to a degree change in flap angle then results in 30% of the average change in normal force due to a degree change in inflow angle. This compares well with the previous results. The results of the step cases are shown in Fig. 7.

$$\frac{\partial F_N}{\partial \delta} = 0.30 \frac{\partial F_N}{\partial \alpha}$$

where F_N the integral normal force on the section, δ the flap angle and α the inflow angle

The final cases concern prescribed azimuth-based flap

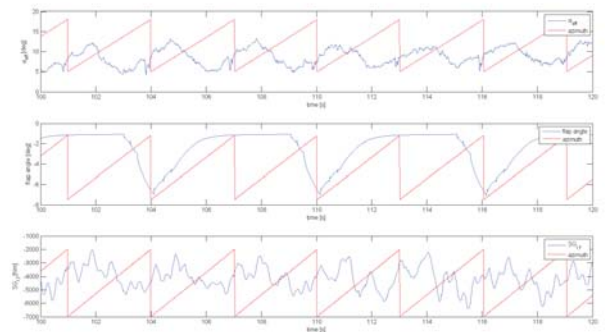


Fig. 8. Time series for flap azimuth control case at 5deg pitch with flap angle to P_{max} (max negative flap deflection) at tower passage (top to bottom: inflow angle, flap angle, root flapwise bending moment).

control, which comprise 10min time series with the flap activated once per revolution towards its maximum positive or negative angles in order to counteract loading fluctuations during the tower passage (downwind configuration). The flap signal is a 0.33Hz harmonic signal (1/rev) with a tuned phase. All cases are run at a pitch setpoint of 5 deg. The flap is scheduled to be active either every second revolution or to be active for 5 revolutions, followed by 5 revolutions without activation. The flap activation comprises an approximate half-sinusoidal signal from almost zero flap angle to either maximum positive or negative flap deflection. In Fig. 8 the time series for a case of azimuthal flap activation towards maximum negative flap deflection during the tower passage every second revolution is shown. The effect of the tower passage in the inflow angle is seen at every revolution, resulting in a variation of the flapwise moment at the boom root. The flap activation affects the fluctuations of the moment. The effect is clearly seen in Fig. 9 where the cycles with flap activation show an increase of the normal force local minimum around the tower passage. The increase of the local normal force results in an increase in the boom root bending moment (reduced bending towards the tower). The opposite behavior is seen for flap activation towards the maximum positive flap deflection.

In the aforementioned cases, the flap is activated every second revolution with no phase difference with the tower passage (0deg./360deg). Other cases have also been tested where the flap is activated with a phase lead of 22.5 deg. before the tower passage, but flap performance was seen to be reduced compared to the 0deg. phase angle. Moreover cases 45-48 comprise the same flap activation at 5 consecutive revolutions instead of every second revolution. No clear trend of affecting loads with flap activation was identified, since due to changing inflow the consecutive cases are not well correlated for a fair comparison. The difference in the statistics of normal force, blade section root flapwise moment and boom root flapwise moment between consecutive revolutions with no flap or flap activation is shown in Fig. 10, Fig. 11, and Fig. 12. The average trend of the flap activation effect on the loads is observed consistently in all plots. Cycles

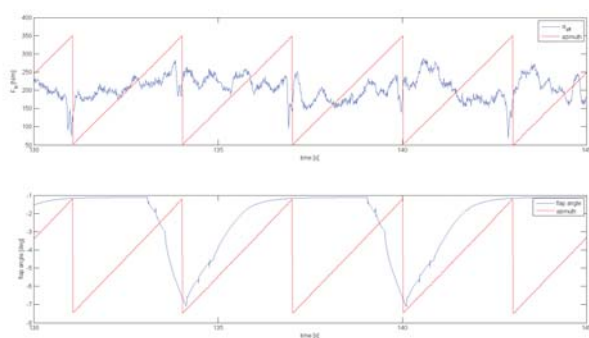


Fig. 9. Time series for flap azimuth control case at 5deg pitch with flap angle to P_{min} (max negative flap deflection) at tower passage (top to bottom: normal force, flap angle).

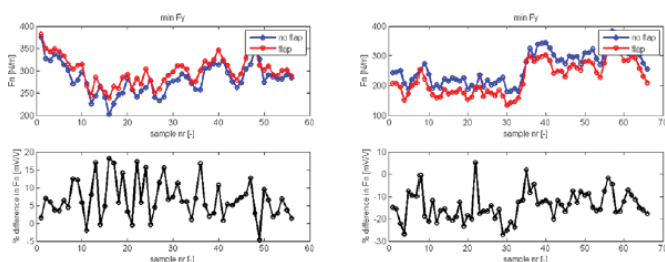


Fig. 10. Comparison of minimum normal force around tower passage between consecutive samples of no flap and flap activation (left: flap to max negative flap angle, right: flap to max positive flap deflection).

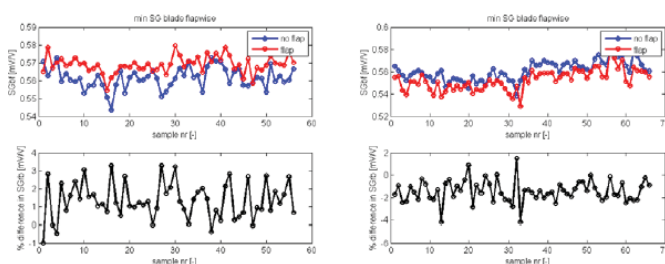


Fig. 11. Comparison of minimum flapwise bending moment at blade section root around tower passage between consecutive samples of no flap and flap activation (left: flap to max negative flap deflection, right: flap to max positive flap deflection).

with flap activation to maximum negative flap deflection show an increase of the normal force local minimum around the tower passage compared to consecutive cycles with no flap. The increase of the local normal force results in an increase in the blade section root flapwise moment and the boom root flapwise moment (reduced bending towards the tower). The opposite behavior is seen for flap activation towards the maximum positive flap deflection. The differences in statistics are shown in Table II. Considerable average reduction of extreme loading in the order of 15% is achieved.

V. CONCLUSION

The tests of a prototype Active Flap System (AFS) are described as performed on the rotating test rig at the Risø

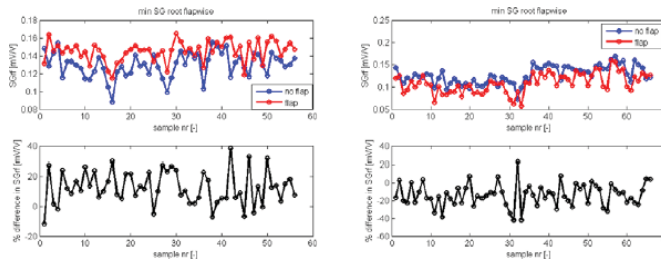


Fig. 12. Comparison of minimum flapwise bending moment at boom root around tower passage between consecutive samples of no flap and flap activation (left: flap to max negative flap angle, right: flap to max positive flap deflection).

case	difference in min FN	difference in min SGbf	difference in min SGrf
max positive flap angle	-14.0	-1.5	-14.0
max negative flap angle	+6.5	+1.5	+12.5

TABLE II

STATISTICS OF FLAP AZIMUTH CONTROL CASES (F_N : NORMAL FORCE, SG_{bf} : BLADE SECTION ROOT FLAPWISE MOMENT, SG_{rf} : BOOM ROOT FLAPWISE MOMENT).

campus of DTU, including an overview of sensors on the setup and the test cases. The post-processing of data is discussed and results of steady, flap step, and azimuth control flap cases are presented. Steady and step case results show the average change in normal force due to a degree change in flap angle then results in 30-32% of the average change in normal force due to a degree change in inflow angle. The azimuth flap control, cases show that a prescribed flap motion once per revolution targeting the inflow fluctuations due to the tower passage can provide an average change of 14% in root moment and sectional force. The tests in general have provided an important proof of concept of the AFS technology in real atmospheric conditions and have validated the flap prototype in terms of aerodynamic performance and load control potential.

ACKNOWLEDGMENT

The work of the following colleagues who have contributed to the design and operation of the flap system and the rotating rig is acknowledged: P. B. Andersen, L. Bergami, J. Christensen, C. Madsen, J. Heininge, M. Markussen, K. Enevoldsen, P. Hansen, K. Clemmensen, M. Rasmussen, L. Christensen, O. Hst, H. Jensen, E. Juul, J. E. Jørgensen, M. Nimb, J. S. Andersen.

The following industrial partners are also acknowledged for their contribution to the flap and powering system design and production: T. Schettler, P. Michels, M. Schoebel (Rehau),

M. Heisterberg (Hydratech Industries), M.B. Christensen.

The research and development work '*INDUFLAP: Industrial adaptation of a prototype flap system for wind turbines*' has been funded by the Danish development and demonstration programme EUDP under contract J.nr. 64010-0458.

REFERENCES

- [1] H A Madsen P B Andersen T L Andersen C Bak and T Buhl, *The potentials of the controllable rubber trailing edge flap*, Proceedings of the EWEC 2010, Warsaw, Poland, 2010.
- [2] H A Madsen P B Andersen T L Andersen C Bak and T Buhl, *Review of state of the art in smart rotor control research for wind turbines*, Prog Aerospace Sci 46 (2010), 1-27, 2010.
- [3] T K Barlas and H A Madsen, *Influence of actuator dynamics on the load reduction potential of wind turbines with distributed controllable rubber trailing edge flaps (CRTEF)*, Proceedings of the 22nd International Conference on the Adaptive Structures and Technologies (ICAST), Corfu, Greece. 2011.
- [4] H A Madsen et al., *Towards an industrial manufactured morphing trailing edge flap system for wind turbines*, Proceedings of the EWEC 2014, Barcelona, Spain, 2014.
- [5] D Castaignet et al., *Full-scale test of trailing edge flaps on a Vestas V27 wind turbine: active load reduction and system identification*, Wind Energy 17 (4), 549564, 2014.

Thanasis K. Barlas Thanasis (Athanasios) K. Barlas is a Dr. Dipl. Eng. Mechanical Engineer who has been active in smart wind turbine blade research for the past 10 years. He graduated from University of Thessaly (UTH) in Greece in 2004, acquired his PhD in Delft University of Technology (TUDelft) in 2011 and pursued his post-doc research at former Risø-DTU (now DTU Wind Energy) in 2011-2012. He has been a research advisor at the Laboratory of Fluid Mechanics and Turbomachinery at the Department of Mechanical Engineering in UTH since 2012. He has served as a private in the Technical Corps of the Greek army in 2012-2013 and later on he worked as a project manager in the Blades Module of Siemens Wind Power in Denmark in 2013-2014. He is currently a researcher at DTU Wind Energy. His main research interests include active aerodynamic control, smart blades, unsteady aerofoil and wake aerodynamics and aeroelasticity.

Helge A. Madsen Helge A. Madsen is a Prof. Dr. MSc Mechanical Engineer who has been active in wind turbine aerodynamics and aeroelasticity research for the past 30 years. He graduated from Aalborg University in Denmark in 1979 and acquired his PhD there in 1983. He has been a scientist, senior scientist, research specialist and currently professor at DTU Wind Energy (formerly Risø National Laboratory, Risø-DTU) since 1984. His main research interests include rotor aerodynamics, aeroelastics and noise and active aerodynamic control.